A New Method to Calculate Relative Distance of Closest Terrain Point Using Interferometric Radar Altimeter Output in Real Flight Environment

Juhyun Oh, Chang-Ky Sung, Jung-Shin Lee, Myeong-Jong Yu
Navigation Sensors & Systems Directorate
Agency for Defense Development
Daejeon, Republic of Korea
juhyunoh@add.re.kr

***Abstract*— Conventional TRN algorithm considered Radar Altimeter (RA) measured altitude, the distance to the closest terrain point within the antenna beam width, as the direct relative altitude below the vehicle. The altitude error occurred in this process resulted in TRN errors. To overcome this drawback of the Rader Altimeter, the Interferometric Radar Altimeter (IRA) was developed jointly by Agency for Defense Development (ADD) and Hanwha Systems. With IRA, more complicated calculation is required to determine the precise relative distance of the closest terrain point using the sensor output. In order to calculate the relative distance to the closest terrain point using the output of the IRA in a real flight environment where the influence of the wind exists, a new approach different from the conventional one is necessary. In this paper, the new relative distance calculation method is proposed for that point, and proved mathematically. To evaluate the accuracy of the proposed approach, flight test was executed and analyzed. The flight test result shows that there was a difference between the Euler angles and the effective observation angles obtained by vehicle's velocity due to wind effects. With the wind effect, the zero Doppler line is located at the skewed position from the aircraft lateral axis, and the difference was confirmed between the proposed closest terrain point calculation method and that of the conventional. The accuracy of each relative distance calculation method was evaluated by comparing the altitude of the closest terrain point and terrain DB obtained by LiDAR(Light Detection and Ranging) during flight test. The new method has smaller mean and standard deviation of the altitude error, implying the superiority of the proposed algorithm.**

Keywords—terrain referenced navigation; interferometric radar altimeter; flight test;

I. INTRODUCTION

Terrain Referenced Navigation (TRN) is one of the navigation technology which estimates vehicle's position by comparing measured terrain elevation below vehicle using a sensor such as Radar Altimeter (RA) when GNSS is unavailable due to hostile jamming [1]. According to the existing research results, the fundamental performance limitations of TRN are database (DB) accuracy and the RA beam width problem [2]. Conventional TRN algorithm considered RA measured altitude, the distance to the closest terrain point within the antenna beam width, as direct relative altitude below the vehicle. The altitude error occurred in this process resulted in TRN performance degradation. To overcome this drawback of the RA, the Interferometric Radar Altimeter (IRA) was developed [3]. The IRA can measure slant range and look angle of the closest terrain point on the zero Doppler line. The TRN systems using IRA can calculate more accurate distance to the closest terrain point using the range and look angle. However, more complicated calculation is required to determine the precise relative distance of closest terrain point using the IRA measurements. There are some papers about TRN using IRA based on simulation [3-5], but ones based on actual flight test results are rare. In order to measure the relative distance of the closest point of the IRA in the actual environment, the influence of the wind must be considered. In this paper, the new relative distance calculation method is proposed, and proved mathematically. To evaluate the accuracy of the proposed approach, flight test was executed and analyzed.

II. INTERFEROMETRIC RADAR ALTIMETER

In order to perform TRN on an aircraft, a RA is needed to measure the altitude between the surface and the aircraft. Conventional TRN algorithm considered RA measured altitude, the distance to the closest terrain point within the antenna beam width, as direct relative altitude below the vehicle. The altitude error occurred in this process resulted in TRN performance degradation. Fig. 1 shows the error examples of the conventional RA. In order to reduce this error, the antenna beam width could be reduced by raising the frequency of the RA. However, even if the antenna beam width is reduced, the fundamental problem, navigation error increases the altitude of the aircraft remained.

On the other hand, IRA can select signals whose Doppler is zero by pulse compressing. In order to obtain the angle of the first returning signal, two or more antennas were placed in the transverse direction of the flight vehicle, and an interferometer method was used [6]. The IRA outputs the slant range(R) to the closest point in the signal reflected from the zero Doppler

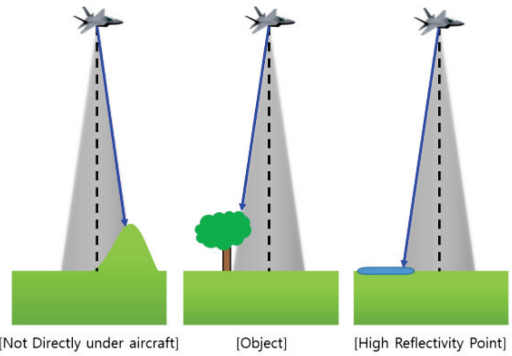

Fig. 1. Error examples of the conventional Radar Altimeter

region and the look angle (θ) in the direction of the transverse axis using the terrain referenced navigation system. Since the IRA outputs the look angle, unavailable in conventional RA, it is possible to measure the horizontal and vertical relative distances from the aircraft to the closest point more precisely.

Agency for Defense Development (ADD) and Hanwha System designed and made this IRA and carried out aircraft mounting tests [7, 8]. Through several flight tests, differences between the actual flight environment and the simulation environment were found. While flying, the attitude of the aircraft and the velocity vector do not match due to the influence of wind. Therefore, a new relative distance measurement method is needed for actual flight environment.

III. Relative distance measurement equation

The horizontal position and altitude of the closest point can be calculated by using the output of the IRA. If the position of the aircraft is $x_k = [x_{k,longitude}, x_{k,latitude}, x_{k,altitude}]^T$ and the relative distance to the closest point is$p_k = [p_{k,longitude}, p_{k,latitude}, p_{k,altitude}]^T$, the position of the closest point is $x_k + p_k$. The TRN algorithm uses the difference between the altitude value of the closest point obtained by the IRA measurement and the terrain DB altitude value of the horizontal point of the closest point as a measurement value.

$$z_k = \left(x_{k,alt} + p_{k,alt}\right) - h_{DEM}\left(x_{k(lat,lon)} + p_{k,(lat,lon)}\right) \quad (1)$$

Where h_{DEM} denotes terrain DB function which computes the elevation of terrain using DEM when the aircraft's lateral position is given.

To obtain the measurements of the TRN algorithm, the relative distance p_k between the aircraft and the closest point should be obtained using the slant range(R) and the look angle (θ) of IRA. The IRA output is information about a point in the zero Doppler region, which is determined by the actual moving direction of the aircraft, that is, the velocity vector.

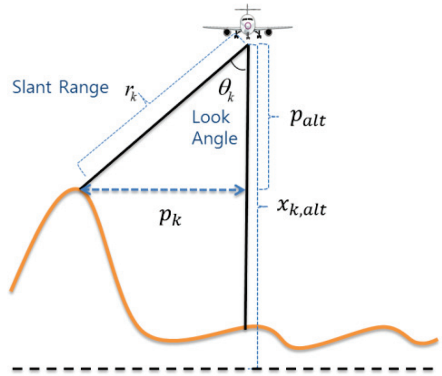

Fig. 2. Measurement model for Interferometric Radar Altimeter in [3]

A. Conventional method 1

In the previous research, the relative distance measurement equation for the closest point is presented as follows [3].

$$p_k = \begin{bmatrix} p_{lon} \\ p_{lat} \\ p_{alt} \end{bmatrix} = \begin{bmatrix} p_e \\ p_n \\ p_u \end{bmatrix} = \begin{bmatrix} r_k sin\theta_k sin\emptyset \\ r_k sin\theta_k cos\emptyset \\ -r_k cos\theta_k \end{bmatrix} \quad (2)$$

Fig. 2 shows the measurement model for IRA in [3]. Using this formula, the relative distance to the closest point is calculated easily using the heading angle when the roll and pitch angles are zero. It also helps when understanding the relative distance between the closest point and the flight vehicle using the IRA Range and look angle. In order to consider the roll angle in this formula additionally, it can be achieved simply by replacing it with the sum of the look angle and roll angle instead of the look angle value. The existing paper [3] does not show how to calculate the closest point when pitch exists, but it can be calculated using the following formula.

$$p_k = \begin{bmatrix} p_{lon} \\ p_{lat} \\ p_{alt} \end{bmatrix} = C_b^n(\gamma + \theta_k, \vartheta, -\psi) \begin{bmatrix} 0 \\ 0 \\ -\mathrm{R} \end{bmatrix} \quad (3)$$

Where, γ, ϑ, ψ are roll, pitch and heading angle of the aircraft, respectively.

$$C_1\ (\phi_z) = \begin{bmatrix} cos\phi_z & sin\phi_z & 0 \\ -sin\phi_z & cos\phi_z & 0 \\ 0 & 0 & 1 \end{bmatrix} \quad (4)$$

$$C_2\ (\phi_x) = \begin{bmatrix} 1 & 0 & 0 \\ 0 & cos\phi_x & sin\phi_x \\ 0 & -sin\phi_x & cos\phi_x \end{bmatrix} \quad (5)$$

$$C_3\ (\phi_y) = \begin{bmatrix} cos\phi_y & 0 & -sin\phi_y \\ 0 & 1 & 0 \\ sin\phi_y & 0 & cos\phi_y \end{bmatrix} \quad (6)$$

$$C_b^n\left(\phi_z, \phi_x, \phi_y\right) = C_1\ (\phi_z) C_2\ (\phi_x) C_3\ (\phi_y) \quad (7)$$

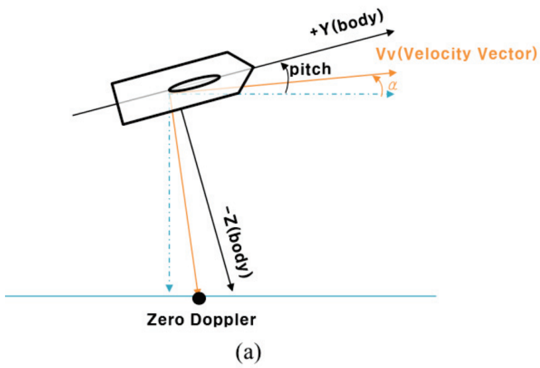

Fig. 3. Comparison between aircraft's attitude and velocity vector in the actual flight environment

In the simulation environment which does not consider wind condition, it is possible to calculate the position of the closest point by the Euler angle, because the angle of Euler angle and the aircraft's velocity vector coincides. However, this formula can't be used in the actual flight environment which has wind effect.

B. Conventional method 2

In another paper, the relative distance to the closest point is calculated by an equation that considers the wind effect in addition to the existing one [1]. Since the subject of the paper was not an IRA relative distance measurement formula, it is not explained in detail. The relative distance measurement formula of the closest point considering wind effect is described in detail as follows.

Fig. 3 shows examples of aircraft's attitude in the actual flight environment. While maintaining the altitude, the aircraft's angle of attack is not 0˚ due to the lift of the air, so the pitch angle is not 0˚(Fig. 3. (a)). In addition, the heading angle of the aircraft may be different from the actual direction of the aircraft by winds blowing from the sides of the aircraft (Fig. 3. (b)). Therefore, in order to measure the relative distance to the closest point, an effective observation angle determined by the velocity vector, is required than the Euler angle. In this paper, effective roll, pitch and heading angle determined by velocity are denoted as ξ, α and β. The effective observation angle α and β can be obtained by the following equation.

$$\alpha = tan^{-1}\frac{v_u}{\sqrt{{v_e}^2+{v_n}^2}} \tag{8}$$

$$\beta = \begin{cases} tan^{-1}\frac{v_e}{v_n} & ,|v_n| \geq |v_e| \\ \frac{\pi}{2} - tan^{-1}\frac{v_n}{v_e} & ,|v_n| < |v_e| \end{cases} \tag{9}$$

For the sake of understanding, the relative distance p from the aircraft to the closest point is shown in Fig. 4. Fig. 5 also shows the result of projecting the Fig. 4 on the East-North plane. The signs of α and β are the same as those of pitch and heading, and the look angle has the opposite sign to roll. In conclusion, the relative position from the aircraft to the closest point is as follows.

$$p = \begin{bmatrix} p_e \\ p_n \\ p_u \end{bmatrix} = \begin{bmatrix} Rcos\theta sin\alpha sin\beta + Rsin\theta cos\beta \\ Rcos\theta sin\alpha cos\beta - Rsin\theta sin\beta \\ -Rcos\theta cos\alpha \end{bmatrix}$$

$$= \mathrm{R}\begin{bmatrix} sin\alpha sin\beta & cos\beta \\ sin\alpha cos\beta & -sin\beta \\ -cos\alpha & 0 \end{bmatrix}\begin{bmatrix} cos\theta \\ sin\theta \end{bmatrix} = RS\begin{bmatrix} cos\theta \\ sin\theta \end{bmatrix} \tag{10}$$

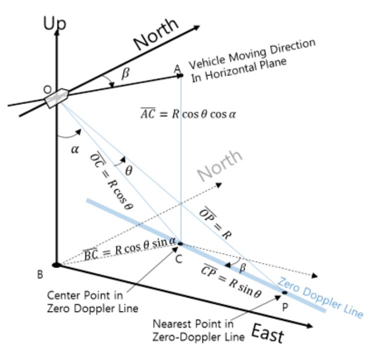

Fig. 4. 3-dimensional graph of the relative distance from aircraft to the closest point.

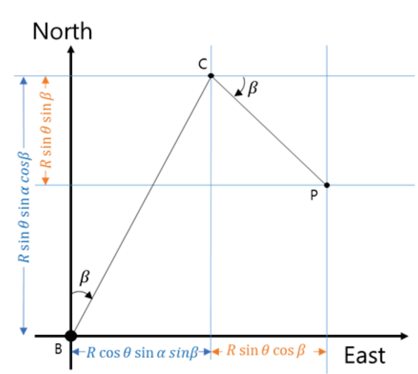

Fig. 5. 2-dimensional graph of the relative distance from aircraft to the closest point on East-North plane.

In the existing paper [1], if the roll angle (γ) is not 0 °, (look angle (θ) + roll angle (γ)) is substituted for look angle (θ).

$$p = \begin{bmatrix} Rcos(\theta+\gamma)sin\alpha sin\beta + Rsin(\theta+\gamma)cos\beta \\ Rcos(\theta+\gamma)sin\alpha cos\beta - Rsin(\theta+\gamma)sin\beta \\ -Rcos(\theta+\gamma)cos\alpha \end{bmatrix} \quad (12)$$

C. Proposed new relative distance measurement equation

The three IRA antennas are arranged side by side along the transverse axis (X axis) of the aircraft as shown in Fig. 6. The IRA's look angle can be obtained using the range measurements between each antenna and the target. See [9] for details on how to compute the look angle using the phase difference between the slant ranges. The look angle of IRA is the angle of measurement based on the downward direction of the vehicle from the center antenna.

However, as described above, the center of zero Doppler line is different from the downward point of aircraft's attitude in actual flight environment. Fig. 7 shows the location of the zero Doppler line on the surface in real flight conditions. The aircraft's heading angle is assumed to be 0˚(North direction) for better understanding, although the influence of the wind exists, and β is not 0˚. Then, the zero Doppler line and the aircraft lateral axis(X axis) are skew lines. We supposed point C is the center of zero Doppler line, and point P is the closest point. In this case, the angle required to calculate the relative position of the actual closest point is ∠COP, but the sum of look angle output from the IRA and roll angle is ∠SOP, which are different from each other in Fig. 7.

The effective roll angle, ξ required to calculate the relative position of the actual point cannot be obtained by the speed of the aircraft as the angles α and β, but can be mathematically derived as follows.

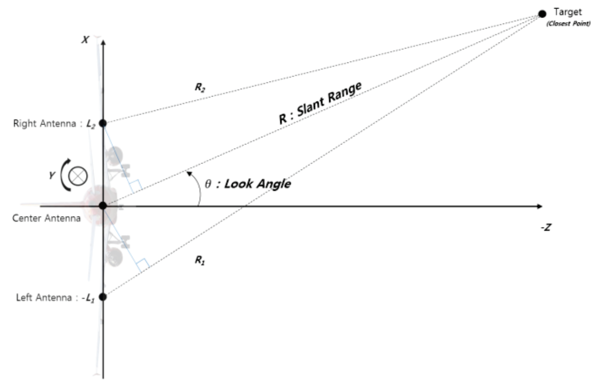

Fig. 6. Look angle measurement of IRA

$x_l^b = [-L_1 \quad 0 \quad 0]^T$: The position of the left antenna in the body frame.

$x_r^b = [+L_2 \quad 0 \quad 0]^T$: The position of the right antenna in the body frame.

$$x_l^n = C_b^n x_l^b, x_r^n = C_b^n x_r^b \quad (12)$$

According to the IRA angle calculation algorithm,

$$\mathrm{R} - \|x_l^n - p\| = L_1 sin\theta \quad (13)$$

$$\|x_r^n - p\| - \mathrm{R} = L_2 sin\theta \quad (14)$$

$$\sqrt{(x_l^n - p)^T(x_l^n - p)} = R - L_1 sin\theta \quad (15)$$

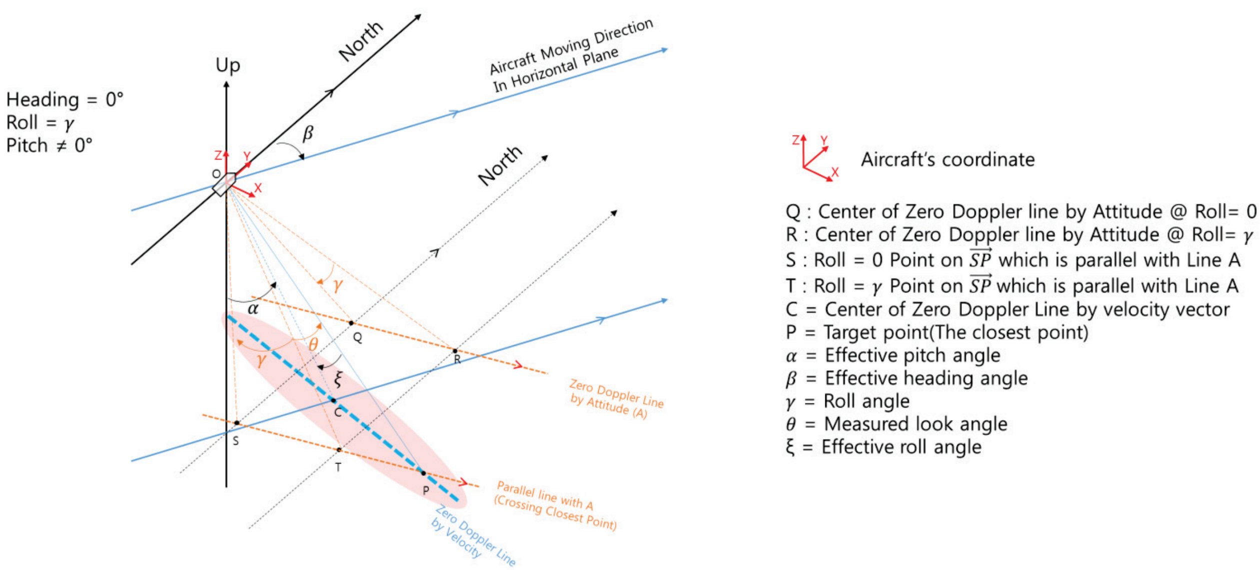

Fig. 7. 3-dimensional graph of the relative distance from aircraft to the closest point in real flight condition.

$$\sqrt{(x_r^n - p)^T (x_r^n - p)} = R + L_2 sin\theta \tag{16}$$

When deployed to the square both sides,

$$L_1^2 - 2{x_l^n}^T p + R^2 = R^2 - 2L_1 sin\theta + L_1^2 sin^2\theta \tag{17}$$

$$L_2^2 - 2{x_r^n}^T p + R^2 = R^2 + 2L_2 sin\theta + L_2^2 sin^2\theta \tag{18}$$

After clearing R^2, divide both sides by R , $L_1 \ll R, L_2 \ll R$

$$\frac{1}{R}{x_l^n}^T p = L_1 sin\theta \tag{19}$$

$$\frac{1}{R}{x_r^n}^T p = -L_2 sin\theta \tag{20}$$

The left sides of the above two equations are

$$\frac{1}{R}{x_l^n}^T p = \frac{1}{R}L_1[-1 \quad 0 \quad 0]C_n^b RS \begin{bmatrix} cos\xi \\ sin\xi \end{bmatrix} \tag{21}$$

$$= L_1[-1 \quad 0 \quad 0]C_n^b S \begin{bmatrix} cos\xi \\ sin\xi \end{bmatrix} \tag{22}$$

$$\frac{1}{R}{x_r^n}^T p = \frac{1}{R}L_2[+1 \quad 0 \quad 0]C_n^b RS \begin{bmatrix} cos\xi \\ sin\xi \end{bmatrix} \tag{23}$$

$$= L_2[+1 \quad 0 \quad 0]C_n^b S \begin{bmatrix} cos\xi \\ sin\xi \end{bmatrix} \tag{24}$$

Therefore, following single expression for ξ is acquired.

$$[-1 \quad 0 \quad 0]C_n^b S \begin{bmatrix} cos\xi \\ sin\xi \end{bmatrix} = [t_1 \quad t_2] \begin{bmatrix} cos\xi \\ sin\xi \end{bmatrix} = sin\theta \tag{25}$$

Dividing both sides by $\sqrt{t_1^2 + t_2^2}$,

$$\frac{t_1}{\sqrt{t_1^2+t_2^2}} cos\xi + \frac{t_2}{\sqrt{t_1^2+t_2^2}} sin\xi = \frac{sin\theta}{\sqrt{t_1^2+t_2^2}} \tag{26}$$

$$sin\eta cos\xi + cos\eta sin\xi = sin(\eta + \xi) = \frac{sin\theta}{\sqrt{t_1^2+t_2^2}} \tag{27}$$

$$\eta + \xi = sin^{-1}\frac{sin\theta}{\sqrt{t_1^2+t_2^2}} \tag{28}$$

$$\xi = sin^{-1}\frac{sin\theta}{\sqrt{t_1^2+t_2^2}} - \eta = sin^{-1}\frac{sin\theta}{\sqrt{t_1^2+t_2^2}} - tan^{-1}\frac{t_1}{t_2} \tag{29}$$

The relative position of the most closest point can be calculated using the derived effective observation angles ξ, α and β as follows.

$$p = \begin{bmatrix} Rcos\xi sin\alpha sin\beta + Rsin\xi cos\beta \\ Rcos\xi sin\alpha cos\beta - Rsin\xi sin\beta \\ -Rcos\xi cos\alpha \end{bmatrix} \tag{30}$$

IV. FLIGHT TEST FOR IRA

A. Preparation

The IRA aircraft test was prepared by referring to the RA aircraft test conducted by ADD [10]. For the aircraft test, civil aircraft of Geostory Corporation, king air e90, was used. The aircraft of Geostory was equipped with LiDAR(Light Detection and Ranging), which can acquire digital terrain map, so it was able to obtain 3m resolution DEM(Digital Elevation Model) and DSM(Digital Surface Model) for the flight area during the aircraft test.

The system configuration used for the IRA aircraft test is shown in Fig. 8. The navigation system consists of Navigation grade Inertial Navigation System (INS) and Global Position System (GPS). Since the navigation system was configured to perform "In Flight Alignment (IFA)", it was possible to obtain accurate position, attitude, and speed. The altitude of the INS was corrected based on the GPS altitude (Mean Sea Level). When performing a real terrain reference navigation, the altitude of the INS is corrected based on the barometric altimeter. In order to evaluate IRA performance precisely, however, GPS correction was applied instead of the barometric altimeter. Since the GPS antenna is installed 2 m above the IRA antenna, the lever arm was compensated after the test. The IRA antenna and INS were installed on the same plate so that their attitudes coincided. The mounting error between the IRA antenna and the INS was measured with a digital level meter within 0.05 degree.

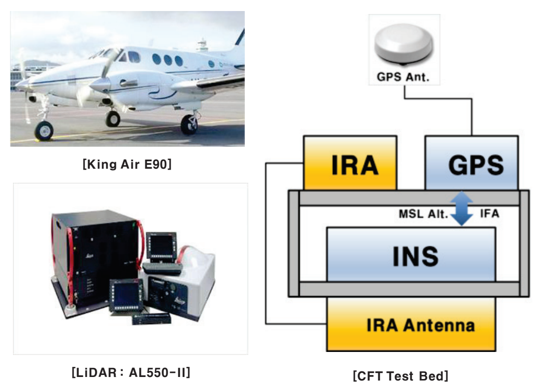

Fig. 8. The system configuration used for the IRA aircraft test

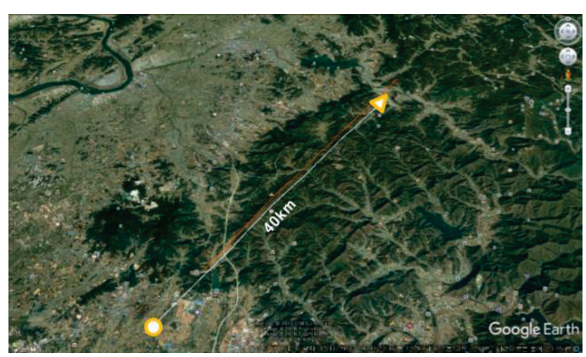

Fig. 9. The flight test trajectory

The flight trajectory for the test was selected in advance as a mountain area (Fig. 9). The average velocity of aircraft was 85m/s, and the flight distance was about 40km.

B. Result

In order to evaluate the performance of IRA, the error was evaluated based on the terrain DB obtained using LiDAR. The error was calculated by (1) and (31). The terrain DB used for the analysis were DEM and DSM with 3m resolution. The hardware and software design of IRA is not fixed yet, so there were some bad measurements in flight test. Result analysis was performed only on normal data with an error of less than 50 m and other data were excluded from the analysis. The analysis results are shown in Fig. 10 and TABLE. 1. The DEM reflects altitude information on the surface of earth from which the feature has been removed. On the other hand, the DSM reflects altitude information including features. Fig. 11 shows the difference between DSM and DEM. As shown in Fig. 10, there were height differences between DSM and DEM as high as trees, because the flight test area was a tree-rich area. As compared with IRA measurement height error by DSM and DEM in the TABLE 1, the error average and standard deviation of DSM is smaller than DEM. In conclusion, it is better to use DSM as terrain DB when using IRA reference. This means that the IRA measures signals reflected from surfaces of objects such as trees, rocks, and buildings rather than the terrain surface. Therefore, the TRN system will get better performance when using DSM than DEM. Therefore, all of following analyzes used DSM as height measurement reference.

As described in Section II, we checked whether the aircraft's attitude (roll, pitch and heading) and the effective observation angle (ξ, α, β) differ from each other when the aircraft is actually flying. Fig. 12 shows comparison graph between aircraft's attitude and the effective observation angle. The change pattern of each angles are almost same. Fig. 13 shows the angle difference between aircraft's attitude and the effective observation angle (Attitude angle - Effective observation angle). As shown in the Fig. 13, the angle difference is exist and not fixed certain value, but changed continuously. The angle difference of pitch is about 1.5 to 2.5 degrees and the heading is about 4 to 5.5 degrees. We confirmed that there is difference between aircraft's attitude and the effective observation angle in real flight environment.

TABLE I. THE HEIGHT ERROR BY EACH TERRAIN DB

Terrain DB type	Height Error(m)	
	Average	*Standard Deviation*
DEM(3m)	12.79	5.33
DSM(3m)	6.99	4.93

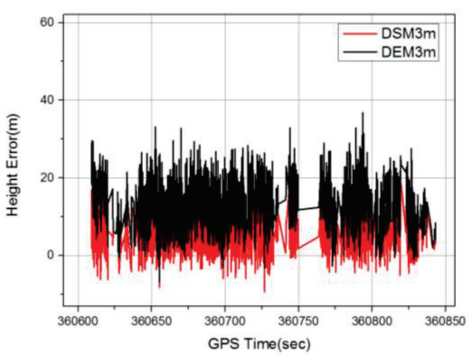

Fig. 10. Comparison of IRA measurement Error by Terrain DB types

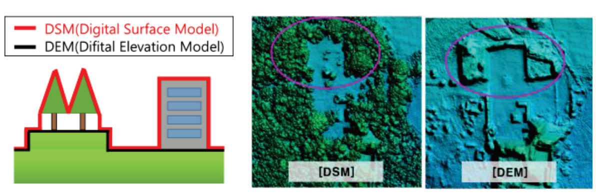

Fig. 11. Difference between DSM and DEM[11]

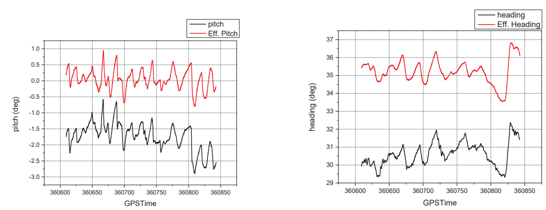

Fig. 12. Comparison graph between aircraft's attitude and the effective observation angle

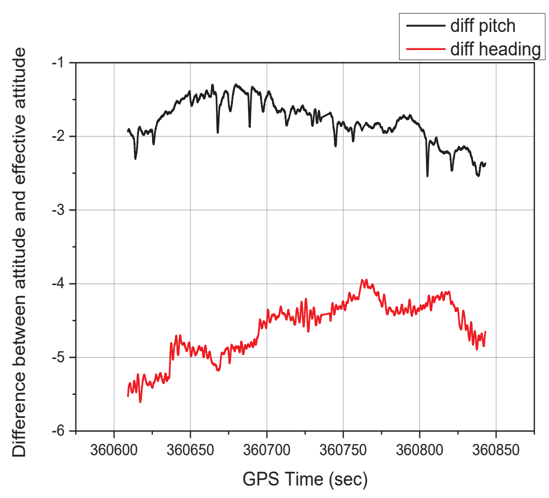

Fig. 13. Angle difference between aircraft's attitude and the effective observation angle

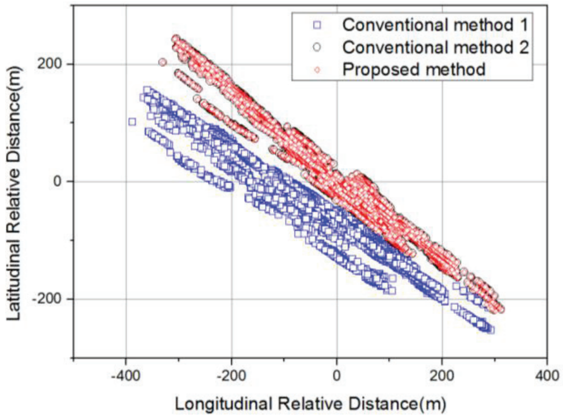

Fig. 14. Comparison of closest points calculated by each method

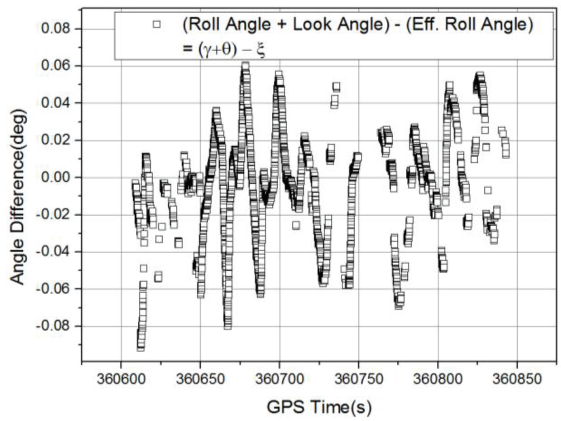

Fig. 15. Difference between angle (γ+θ) and ξ

Fig. 14 shows comparison of closest points calculated by each method described in Section III. Conventional method 1 considered the zero Doppler line to be drawn at the heading angle, and conventional method 2 and proposed method were considered to be drawn at the effective heading angle. Therefore, the positions of the closest points found are different from each other. The difference between conventional method 2 and proposed method is not well identified in Fig 14. The difference between the two formulas is whether to use (γ+θ) or ξ in the formula for finding the closest point. Fig. 15 shows the difference between angle (γ+θ) and ξ. The difference was between -0.1 and 0.06 degrees. This difference causes a closest point horizontal distance error of about 1.7 m at a distance of 1 km (1000m * tan (0.1°) ≒ 1.7m).

The horizontal distance error between the closest points found by the conventional method and the closest points found by the new calculation formula is expressed as shown in Fig 16. Since the aircraft's altitude was 2km during the flight test, the horizontal distance error due to the difference between the two closest point calculation methods was not very large. However, when the altitude is higher, it is expected that the horizontal distance error of the closest point will become more severe.

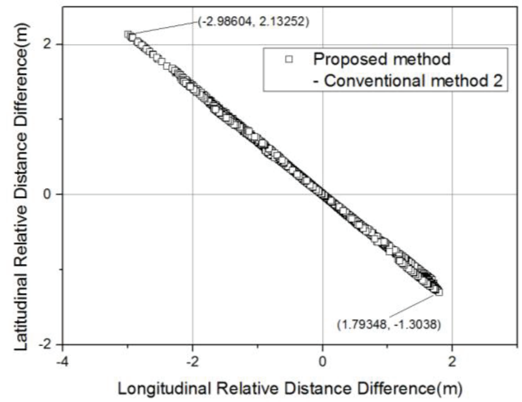

Fig. 16. Horizontal distance Error between the closest points found by conventional method 2 and the closest points found by proposed method

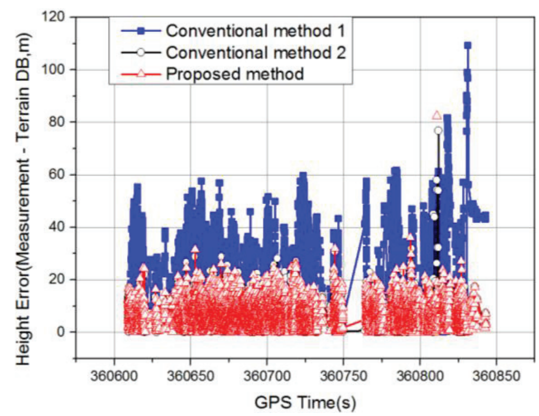

Fig. 17. Comparison IRA measurement errors in each method

TABLE II. THE HEIGHT ERROR BY EACH CALULATION METHOD

Calculation method	Height Error(m)	
	Average	***Standard Deviation***
Conventional method 1	20.91	14.43
Conventional mothod 2	7.71	4.68
Proposed method	7.18	4.63

Fig. 17 and TABLE 2 compare the IRA measurement height error by each calculation method. Through these data, we have obtained the following conclusions. First, the error of conventional method 1 is larger than others. It means that zero Doppler line is determined by aircraft's velocity vector (effective observation angle), not aircraft's attitude. Second, the error of proposed method is smaller than conventional method 2. It means that we need to use effective roll angle ξ to find closest point, than the sum of roll angle and measured look angle(γ+θ).

CONCLUSION

In this paper, a new method to calculate relative distance of closest terrain point using IRA output in real flight environment was proposed and proved mathematically. The new method requires the aircraft's effective observation angles which are determined by the aircraft's velocity vector. In order to evaluate the accuracy of the proposed approach, flight test was executed and analyzed. Flight test result shows that the new method has smaller mean and standard deviation of the altitude error, implying the superiority of the proposed algorithm.

REFERENCES

[1] Sung Chang-Ky, Nam Seong-Ho, Yu Myeong-Jong, "Terrain Referenced Navigation Based on Robust Point Mass Filter Using Variance Adjusted Discrete Normal PDF and Mean Valued Likelihood", Proceedings of the ION 2017 Pacific PNT Meeting, Honolulu, Hawaii, May 2017, pp 126-136

[2] P. D. Groves, Principles of GNSS, Inertial, and Multisensor Integrated Navigation Systems. MA:Artech House, 2008.

[3] S.H. Jung, J.H. Yoon, M.G. Park, D.Y. Kim, C.K. Sung, H.S. Kim, Y.H. Kim, H.J. Kwak, W. Sun, and K.J. Yoon, "A Performance Analysis of Terrain-Aided Navigation(TAN) Algorighms Using Interferometric Radar Altimeter", Journal of The Korean Society for Aeronautical & Space Sciences, vol.40, no.4, Apr. 2012., pp.285-291

[4] Youngjoo Kim, Hyochoong Bang, "A New Measurement Model of Interferometric Radar Altimeter for Terrain Referenced Navigation using Particle Filter", Signals and Systems (ICSigSys) 2017 International Conference on, 2017, pp. 67-71.

[5] Kim, Hyun-suk, et al. "Simulation for the TRN using Interferometric Radar Altimeter and PMF", The Korean Society for Aeronautical and Space Sciences Spring Conference, 2011, pp. 212-216

[6] Inchan Paek, Sangil Lee, Kyungju Yoo, Jong Hun Jang, "An Implemetation of Interferometric Radar Altimeter Simulator", The Jounal of Korean Institute of Electromagnetic Engineering and Science, Jan. 2015, vo.26, no.1, pp. 81-87

[7] Jong Hun Jang, Jong Soo Ha, Young Sik Park, Jin Eep Roh, "Design of an Interferometric Radar Altimeter", The Korean Society for Aeronautical and Space Sciences Fall Conference, 2016, pp. 265-266

[8] Ji An Park, Jihyung Kim, Jae Hyeon Bae, Chan-Bae Kim, Inchan Paek, Man-Gyu Lee, Jong Hun Jang, "Flight test and Results Analysis of the Interferometry Radar Altimeter", The Korean Society for Aeronautical and Space Sciences Fall Conference, 2016, pp. 267-268

[9] Dong-Taek Lee, Hyung-Sup Jung, Geun-Won Yoon, Du-Ra Kim and Woong Sun, "Extraction of Accurate 3-D Ground Coordinates from Interferometric Radar Altimeter(IRA)", 2011 3rd International Asia-Pacific Conference on Systhetic Apeerture Radar(APSAR), Seoul, 2011, pp. 1-4

[10] Jongsuk Yoon, Hee Junn Kwak, Yoon Hyoung Kim, Young Jong Shin, Ki Jeong Yoo and Myeong Jong Yu, "The Performance Analysis of an Airborne Radar Altimeter based on Simultaneously Acquired LiDAR Data", Korean Journal of Remote Sensing, Vol.29, No.1, 2013, pp.81-94

[11] Jennifer von Schwerin, Heather Richards-Rissetto, Fabio Remondino, Maria Grazia Spera, Michael Auer, Nicolas Bilen, Lukas Loos, Laura Stelson, Markus Reindel, "Airborne LiDAR acquisition, post-processing and accuracy checking for a 3D WebGIS of Copan, Honduras", Journal of Archaelological Science : Reports, Vol. 5, Feb. 2016, pp 85-104.